PROCEEDINGS OF SPIE

SPIEDigitalLibrary.org/conference-proceedings-of-spie

Heterodyne instrumentation upgrade at the Caltech Submillimeter Observatory

Jacob W. Kooi, Attila Kovacs, Bruce Bumble, Goutam Chattopadhyay, Michael L. Edgar, et al.

Jacob W. Kooi, Attila Kovacs, Bruce Bumble, Goutam Chattopadhyay, Michael L. Edgar, Steve Kaye, Rick LeDuc, Jonas Zmuidzinas, Thomas G. Phillips, "Heterodyne instrumentation upgrade at the Caltech Submillimeter Observatory," Proc. SPIE 5498, Millimeter and Submillimeter Detectors for Astronomy II, (8 October 2004); doi: 10.1117/12.552539

SPIE.

Event: SPIE Astronomical Telescopes + Instrumentation, 2004, Glasgow, United Kingdom

Heterodyne Instrumentation Upgrade at the Caltech Submillimeter Observatory

J. W. Kooi[1], A. Kovács[1], B. Bumble[2], G. Chattopadhyay[1], M. L. Edgar[1], S. Kaye[1], R. LeDuc[2], J. Zmuidzinas[1], and T. G. Phillips[1]

[1]California Institute of Technology, MS 320-47 Pasadena, California 91125, USA.
[2]Center for Space Microelectronics Technology/JPL, Pasadena, CA 91108

ABSTRACT

Balanced receivers are under development at the Caltech Submillimeter Observatory (CSO) for the 230/460 GHz and 345/660 GHz atmospheric windows. The mixers are tunerless, implemented in a balanced configuration, have a 4-8 GHz IF, and can be used in dual frequency observation mode. As shall be seen, the balanced arrangement provides a high level of amplitude noise immunity and allows all of the available LO power to be used. In turn, this permits complete automation of the receivers by means of synthesized LO source(s). A disadvantage of balanced mixers is, perhaps, that the sidebands at the IF remain convolved (DSB), unlike sideband separating (2SB) receivers. The latter, however are unbalanced and do not have the noise and LO injection advantages of balanced mixers. For the CSO, balanced mixers covering the range 180-720 GHz were judged most promising to facilitate many of the astrophysical science goals in the years to come.

In parallel, a dual polarization 280-420 GHz continuous comparison (correlation) receiver is in an advanced state of development. The instrument has two beams on the sky; a reference and a signal beam. Using only cooled reflecting optics, two polarizing grids, and a quadrature hybrid coupler, the sky beams are coupled to four tunerless SIS mixers (both polarizations). The 4-12 GHz mixer IF outputs are, after amplification, correlated against each other. In principle, this technique results in flat baselines with very low RMS noise, and is especially well suited for high redshift Galaxy work.

Not only do these changes greatly enhance the spectroscopic capabilities of the CSO, they will also enable the observatory to be integrated into the Harvard-Smithsonian Submillimeter Array (SMA), as an additional telescope.

Keywords: Balanced mixer theory, continuous comparison receiver, radial probe, full-height waveguide to thin-film microstrip transition, split-block, high current density superconducting-insulating-superconducting (SIS) tunnel junction, broad bandwidth quadrature waveguide hybrid, DC-break, IF match, Wilkinson in phase power combiner, Low noise amplfier (LNA), 4-8 GHz intermediate frequency (IF).

1. INTRODUCTION

Except for the 800-950 GHz Quasi-Optical receiver, the existing SIS waveguide receivers at the CSO all use waveguide tuners to achieve sensitivities a few times the quantum noise limit. Each of these receivers has played a pioneering role in the submillimeter field. However modern astronomy is demanding more capability in terms of sensitivity, bandwidth, stability, and ease of use. To fulfill this requirement, we are planning a significant upgrade to these instruments. Four tunerless balanced waveguide receivers have been designed to cover the entire 180-720 GHz frequency range. The IF bandwidth of the CSO receivers will increase from the current 1 GHz to 4 GHz, and interface to a newly acquired 4x1 GHz wide bandwidth Acousto-Optical Spectrometer (AOS),[1–3] build by the University of Köln. Dual frequency (2 color) observations in the 230/460 GHz and 345/660 GHz atmospheric frequency bands can be configured by routing the respective receiver IF output(s) to the Köln built hybrid AOS. Not only does this scheme provide a new mode of observation for the CSO, it will also facilitate pointing the telescope in mediocre weather.

Further author information: (Send correspondence to Jacob W. Kooi)
Jacob W. Kooi E-mail: kooi@submm.caltech.edu, Telephone: 1 626 395 4286

Millimeter and Submillimeter Detectors for Astronomy II, edited by Jonas Zmuidzinas, Wayne S. Holland, Stafford Withington, Proceedings of SPIE Vol. 5498 (SPIE, Bellingham, WA, 2004) · 0277-786X/04/$15 · doi: 10.1117/12.552539

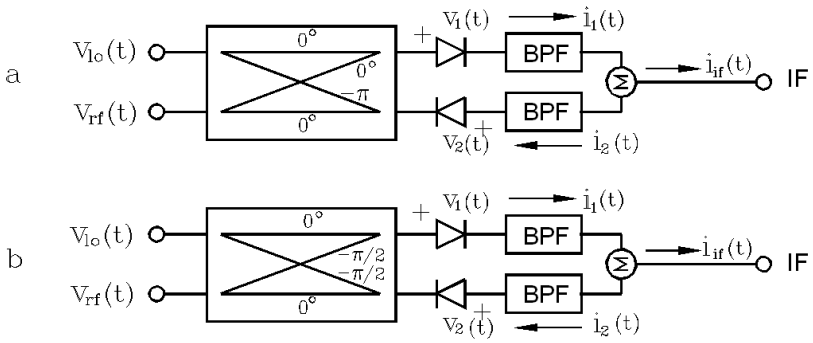

Figure 1. LO and RF currents in a single (2-diode) balanced mixer. In practice, the summing node in the IF can be implemented with a Wilkinson[4] in phase power combiner. In our design, all the circuitry is planar and has been designed using Ansoft's linear circuit and 3D Electromagnetic simulator (HFSS). In the case of the CSO mixers, the IF band pass filter (BPF) is 3-9 GHz.

In addition to the new balanced receivers, we are constructing a specialized 4-channel, dual polarization, continuous comparison (correlation) receiver to operate in the 280-420 GHz atmospheric window. For the back-end correlator, we anticipate using WASP,[5,6] a 16 MHz/channel analog spectrometer from the University of Maryland. The described balanced mixers and the specialized correlation receiver have much of their hardware in common. Design of the mixer blocks, SIS junctions, and the IF amplifier chain is now complete. Delivery of balanced mixer components is expected by winter 2004. The SIS tunnel junctions needed for the upgrade have been developed by Kovács *et. al.* using Supermix,[7] a Caltech developed C^{++} software library for high-frequency (superconducting) circuit simulations. SIS tunnel junction designs were submitted to JPL for fabrication in the spring of 2003 and have since been delivered. Installation of the new instrumentation is anticipated to commence toward the end of 2004. In addition to the 180-720 GHz balanced receivers, an upgrade is planned for the NbTiN quasi-optical twin-slot receiver IF, from the current 1 GHz to 4 GHz.

2. BALANCED MIXER THEORY AND DEVELOPMENT

In principal, a singly balanced mixer can be formed by connecting two reverse biased mixers to a 180° or 90° input hybrid, as shown in Fig. 1.

Quantitatively, we can use an exponential to describe the non-linearity of a diode mixer.[8] It should be noted that SIS tunnel diodes have very sharp I/V curves when compared to Schottky diodes, and can by their quantum mechanical nature exhibit unity or even positive gain. However, in principal this ought not to make a difference in the fundamental performance of the singly balanced mixer under discussion. Using a polynomial series to represent the exponential current i_1 through diode 1 we find

$$i_1(t) = a_0 + a_1 v_1(t) + \frac{a_2 v_1(t)^2}{2!} + \frac{a_3 v_1(t)^3}{3!} \cdots = \sum_{n=0}^{\infty} \frac{a_n v(t)_1^n}{n!}. \tag{1}$$

Because the voltage across diode 2 is reversed from diode 1, e.g. $v_2(t) = -v_1(t)$, we find

$$i_2(t) = b_0 - b_1 v_2(t) + \frac{b_2 v_2(t)^2}{2!} - \frac{b_3 v_2(t)^3}{3!} \cdots = \sum_{n=0}^{\infty} (-1)^n \frac{b_n v_2(t)^n}{n!}. \tag{2}$$

Here a_n and b_n present the mixer conversion gain terms. From Eqn's 1 and 2 we observe that the term n=0 yields the DC component, n=1 the fundamentals, n=2 the second order difference and product terms, and n=3 the harmonic and intermodulation products. Of course for submillimeter or teraherz mixers, the intermodulation product maybe ignored. It is nevertheless interesting to consider the effect from an theoretical point of view. It should also be noted from (1) and (2) that the product terms decrease by n!. Thus we will not consider the fourth order term.

2.1. Singly Balanced Mixer Consisting of a 180° Input Hybrid

In the case of a 180° input hybrid we find

$$v_1(t) = \frac{1}{2}[V_{rf} \cdot e^{i\omega_{rf}t} + V_{lo} \cdot e^{im\omega_{lo}t}], \qquad \rightarrow \ \rightarrow \tag{3}$$

where m presents the LO harmonics $1, 2, 3....$ In the equations, zero phase is indicated by a right arrow. The voltage across diode 2 is seen to be

$$v_2(t) = \frac{1}{2}[V_{rf} \cdot e^{i\omega_{rf}t} - V_{lo} \cdot e^{im\omega_{lo}t}]. \qquad \rightarrow \ \leftarrow \tag{4}$$

At the summing node (ignoring device capacitance and IF bandpass filter) we find the IF current,

$$i_{if}(t) = i_1(t) - i_2(t). \tag{5}$$

Substituting Equation (3) into (1) and Equation (4) into (2), and solving for i_{if}(t) under the assumption that the mixer gain terms $a_n \equiv b_n$, we find for a perfectly balanced mixer, with an 180° input hybrid that,

$$i_{if}(t) = \begin{cases} a_1 V_{rf} \cdot e^{i\omega_{rf}t} + \\ \frac{a_2}{2!}[V_{rf}V_{lo} \cdot e^{i\omega_{rf}t} \cdot e^{im\omega_{lo}t}] + \\ \frac{a_3}{4 \cdot 3!}[V_{rf}^3 \cdot e^{i3\omega_{rf}t} + 3V_{rf}V_{lo}^2 \cdot e^{i(\omega_{rf}+2m\omega_{lo})t}]. \end{cases} \tag{6}$$

The first term is the RF signal, which is deeply embedded in noise for radio-astronomical receivers. The second (product) term yields the sum and difference frequencies of the RF and LO signal, i.e. the IF. The third term is found to yield the RF third harmonic and intermodulation component ($2m\nu_{lo} - \nu_{rf}$, $m = 1, 2, 3, ...$). Note that the intermodulation component is not entirely eliminated in the case of a singly balanced mixer. Of course for submillimeter or terahertz mixers all but the difference product terms are negligible due to inherent device capacitance.

2.2. Amplitude Noise Immunity in the Case of a 180° Input Hybrid

Consider an amplitude modulated signal $V_n \cdot e^{i\omega_n t}$ that along with the LO signal is incident on the LO port of an ideal 180° hybrid. The output of the hybrid yields the following voltages across the two diodes,

$$v_1(t) = \frac{1}{2}[V_n \cdot e^{i\omega_n t} + V_{lo} \cdot e^{im\omega_{lo}t}], \qquad \rightarrow \ \rightarrow \tag{7}$$

and

$$v_2(t) = \frac{1}{2}[V_n \cdot e^{i(\omega_n t - \pi)} + V_{lo} \cdot e^{i(m\omega_{lo}t - \pi)}]. \qquad \leftarrow \ \leftarrow \tag{8}$$

Substituting $v_1(t)$ and $v_2(t)$ in Equation (1) and (2), and solving for $i_{if}(t)$ (5), we find the IF current $\rightarrow 0$ for a 180° balanced mixer. In other words, amplitude noise in an ideal 180° based balanced mixer is seen to cancel perfectly. Of course, a perfect balanced mixer does not exist, especially in the submillimeter or terahertz regimes. Hence it is constructive to analyze the response for a "non-deal" case.

Consider a balanced mixer with unequal gain and phase response. In general, gain imbalance at the IF summing node can result from imbalance in the hybrid (G_h) and/or different conversion gains (a_2, b_2) between the two mixer elements (for example non-identical I/V curves). The phase difference in path length ($\Delta\theta$) is primarily determined by the mounting accuracy of the two (SIS) mixer chips. The level of noise rejection at the IF summing node can be found by taking the ratio of $i_1(t)$ over $i_2(t)$ such that,

$$\frac{i_1(t)}{i_2(t)} = \frac{a_2}{b_2}\sqrt{G_h}\cos(\Delta\theta). \tag{9}$$

If G_m equals the mixer gain imbalance ($a2/b2$), then the noise rejection of a balanced mixer may be defined as,

$$NR = 20 \cdot log\Big[1 - G_m\sqrt{G_h}\cos(\Delta\theta)\Big]. \tag{10}$$

If, for example, in a worst case scenario, the imbalance in the 180° hybrid is 1.5 dB (G_h=0.841), the mixer conversion gain imbalance 2 dB (0.79), and the phase error between the two IF ports is 10 degrees, then the amplitude noise rejection of the singly balanced mixer will be $\approx$ 11 dB.

2.3. Singly Balanced Mixer Consisting of a 90° Input Hybrid

Balanced mixers based on 180° input hybrid circuitry have certain advantages over quadrature hybrid (90°) balanced mixers. The most important characteristics are better LO-RF isolation and harmonic intermodulation product suppression. Unfortunately, 180° hybrids are large (Rat-Race baluns) or difficult to fabricate at frequencies above a few hundred GHz (Wg Magic-Tee). The analysis presented here evaluates the quadrature 2-diode singly balanced mixer. Following a similar analysis to that of with the 180° input hybrid, we define the RF and LO voltages at the input of the quadrature hybrid as (Fig. 1).

$$v_{lo}(t) = V_{lo} \cdot e^{i(m\omega_{lo}t - \pi/2)}, \tag{11}$$

and

$$v_{rf}(t) = V_{rf} \cdot e^{i\omega_{rf}t}. \tag{12}$$

For mathematical simplicity, we use an arbitrary LO phase of $-\pi/2$. Voltages at the output of the quadrature hybrid are thus found to be,

$$v_1(t) = \frac{1}{2}[V_{lo} \cdot e^{i(m\omega_{lo}t - \pi/2)} + V_{rf} \cdot e^{i(\omega_{rf}t - \pi/2)}], \qquad \downarrow \ \downarrow \tag{13}$$

and

$$v_2(t) = \frac{1}{2}[V_{lo} \cdot e^{i(m\omega_{lo}t - \pi)} + V_{rf} \cdot e^{i\omega_{rf}t}]. \qquad \leftarrow \ \rightarrow \tag{14}$$

where m presents the LO harmonics $1, 2, 3....$ Note that in $v_1(t)$, the LO and RF voltages are 180° out of phase, whereas in $v_2(t)$ the LO and RF voltages are in phase, as would be expected. Substituting Equations (13) and (14) into (1) and (2), and summing the IF currents, as in Equation (5), yields

$$i_{if}(t) = \begin{cases} \frac{a1}{\sqrt{2}}[V_{rf} \cdot e^{i(\omega_{rf}t - \pi/4)} - V_{lo} \cdot e^{i(m\omega_{lo}t + \pi/4)}] + \\ \frac{a2}{2!}[V_{lo}V_{rf} \cdot e^{im\omega_{lo}t} \cdot e^{i\omega_{rf}t}] + \\ \frac{a3\sqrt{2}e^{i\pi/4}}{8\cdot 3!}[V_{rf}^3 e^{i3\omega_{rf}t} + 3V_{lo}^2 V_{rf} e^{i(2m\omega_{lo} + \omega_{rf})t} - 3iV_{lo}V_{rf}^2 e^{i(2\omega_{rf} + m\omega_{lo})t} - iV_{lo}^3 e^{i3\omega_{lo}t}]. \end{cases} \tag{15}$$

As before, the fundamental, harmonic, and intermodulation products are severely attenuated by the inherent device capacitance of the submillimeter or terahertz mixing element. It is, however, constructive to observe the difference between the 180° and 90° hybrid balanced mixers. In general, the 180° balanced mixer has superior fundamental and intermodulation product suppression capabilities, which explains the popularity of the 180° hybrid at microwave frequencies. However at frequencies $\gg$ 100 GHz this advantage greatly reduced. For this reason, submillimeter or terahertz mixers may be configured with quadrature hybrids, rather than the larger

and more complex 180° hybrids. Of special interest is the second order term in Eqn. 15. By taking the real part with $m = 1$, it follows that the IF current simplifies to,

$$i_{if}(t) = \frac{a2}{2!} V_{lo} V_{rf} \cos(|(\omega_{lo} - \omega_{rf})t|). \tag{16}$$

Where $a2$ presents the system gain assumimg that the hybrid and mixers are perfectly balanced. This is the same result as obtained in the case for the 180° balanced mixer (Eqn. 6).

2.4. Amplitude Noise Immunity in the Case of a 90° Input Hybrid

Again, consider an amplitude modulated (noise) signal, $V_n \cdot e^{i(\omega_n t - \pi/2)}$, which along with the LO signal is incident on the LO port of the 90° hybrid. The output of the hybrid yields the following voltages,

$$v_1(t) = \frac{1}{2}[V_n \cdot e^{i(\omega_n t - \pi/2)} + V_{lo} \cdot e^{i(m\omega_{lo} t - \pi/2)}], \qquad \downarrow \ \downarrow \tag{17}$$

and

$$v_2(t) = \frac{1}{2}[V_n \cdot e^{i(\omega_n t - \pi)} + V_{lo} \cdot e^{i(m\omega_{lo} t - \pi)}]. \qquad \leftarrow \ \leftarrow \tag{18}$$

Substituting $v_1(t)$ and $v_2(t)$ into Equation (1) and (2), and solving for i_{if}(t) we find

$$i_{if}(t) = \begin{cases} \frac{-a1}{\sqrt{2}}[V_{lo} \cdot e^{i(m\omega_{lo} t + \pi/4)} + V_n \cdot e^{i(\omega_n t + \pi/4)}] + \\ 0 + \\ \frac{a3\sqrt{2}e^{-i\pi/2}}{8 \cdot 3!}[V_{rf}^3 e^{i3\omega_{rf} t} + 3V_{lo}^2 V_{rf} e^{i(2m\omega_{lo} + \omega_{rf})t} + 3V_{lo} V_{rf}^2 e^{i(2\omega_{rf} + m\omega_{lo})t} + V_{lo}^3 e^{i3\omega_{lo} t}]. \end{cases} \tag{19}$$

It is evident that for an ideal quadrature hybrid balanced mixer, only the second order product term (IF) provides "perfect" amplitude noise cancelation. Unlike the ideal 180° singly balanced mixer, the fundamental and third (odd) order modulation noise products remain. Fortunately, at submillimeter frequencies these terms vanish due to the inhererent device capacitance of the mixer (Fig. 1). Of course, a perfect balanced mixer does not exist, especially in the submillimeter or terahertz regime. Hence, it is constructive to analyze the response for a non-perfect scenario.

Following the similar analysis as for the 180° balanced mixer, we write $v_1(t)$ and $v_2(t)$ to include unequal hybrid gain (G_h), mixer conversion gain (a_2, b_2), and phase imbalance $\Delta\theta = |\theta 1 - \theta 2|$. After the band pass filter (BPF) and summing node we again find the reduction in amplitude noise at the IF as,

$$NR = 20 \cdot log\Big[1 - G_m \sqrt{G_h} \cos(\Delta\theta)\Big]. \tag{20}$$

2.5. Physical Implementation of the balanced receivers

The proposed balanced receivers have a 4-8 GHz IF, and are implemented in (tunerless) full height waveguide[13] to minimize RF loss and fabrication difficulties. Four frequency bands are used to cover the 180-720 GHz atmospheric window: 180-280 GHz, 280-420 GHz, 380-520 GHz, 580-720 GHz. To supply the needed LO pump power, planar multiplier sources[9] will be mounted inside the cryostat at the 15 Kelvin stage. This has the advantage of an $\approx 50\%$ increase in available LO power over room temperature operating multipliers. It also greatly reduces complexity in the optics, and improves reliability of the multipliers. We calculate[7] that each SIS junction requires roughly 1 μW of pump power ($\alpha = eV_{lo}/h\nu \approx 1$ on average). Because two SIS junctions are used in a singly balanced mixer configuration, we require 2 μW of LO pump power at the mixer LO input port. In actual fact the LO power requirement is slighly higher due to Ohmic loss in the waveguide internal to the mixer. Since a broad bandwidth cooled multiplier[9] produces at least 70 μW of LO power over the descibed frequency bands, it is neccessary to add (fixed) attenuation in the LO-mixer path. In practice, this is most easily done

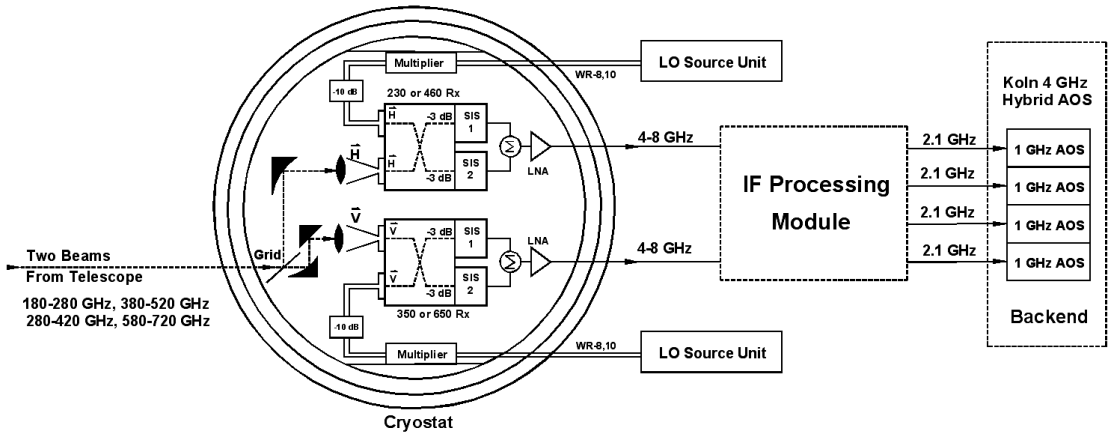

Figure 2. Block diagram of the CSO Facility Instrumentation upgrade to balanced mixers. The LO source signal (70-140 GHz) enters the dewar via a stainless steel waveguide. The tunerless multipliers are mounted on the 15K stage of a hybrid cryostat. This has the advantage of not only simplifying the optics, but also increasing the overall reliability and available LO power ($\approx$ 50%). The LO signals enter the balanced mixers via a cold 8-13 dB directional coupler. This is necessary to minimize standing waves in the LO-Mixer path, and to reduce the available LO power at the mixer ($\approx 2\ \mu$W). The LO noise contribution is estimated, given a (calculated) balanced mixer noise immunity of about 11 dB, to be 0.1K with this scheme. In the event synthesized LO sources are used, Lo noise is expected to increase to a few Kelvin at most. Each cryostat receives two (orthogonally polarized) beams from the sky, which are routed via a cold wire-grid to the appropriate mixer. This technique facilitates dual frequency (2 color) observations, which improves observing efficiency and significantly assists pointing with the high frequency receivers in mediocre weather.

with a directional coupler. The net effect is a reduction in LO noise and standing waves between the multiplier and mixer. In the event a synthesized source (potential for high am, fm and spurious noise) is used to drive the multiplier(s), the addition of a cold attenuator will likely prove to be of great value. An additional reduction in LO noise is provided by the "noise canceling properties" of the balanced mixer. Given an (calculated) amplitude noise rejection of 11 dB (Section 2.4) we estimate that a phase locked Gunn Oscilator source has an amplitude noise contribution of just 0.1 kelvin. The use of a synthesized source is like to increase this value to a few Kelvin, still a very small fraction of the overall receiver noise budget.

Accompanying these new mixers, is a bias control scheme that allows remote control of the instruments. An identical bias scheme is planned for the CASIMIR instrument on SOFIA.[14] An added advantage of this type of receiver configuration, is that it requires minimal changes to the existing cryostat, telescope optics, and some of the LO hardware. Because the Köln AOS consists of four 1 GHz wide AOS channels, the IF bandwidth of each of the two receivers can be configured to use 25, 50, or 100% of the available 4 GHz AOS band. This scheme has the advantage of potentially doubling the observing throughput, as well as having co-aligned beams on the sky. The latter reduces calibration and pointing difficulties, especially for the high frequency receivers in mediocre weather.

3. A 280-420 GHZ DUAL POLARIZATION, CONTINUOUS COMPARISON (CORRELATION) RECEIVER

Probably the most popular receiver at the CSO is the facility 280-420 GHz system. However, for many distant galaxy projects, an improvement in sensitivity of a factor of 5-6 is needed. This can only be obtained by use of a more sophisticated design. This is best achieved by constructing a 4-detector receiver with dual polarization and on-off source detectors operating in a correlation or continuous comparison mode (Predmore *et al.* 1985 [10]). This design rejects signals present in both channels. The block diagram for one polarization of this design is shown in Fig. 3.

It is expected that the rejection of gain variation, plus the extra signal from continuous comparison and dual polarization, will provide a gain in sensitivity of approximately 6 over the existing waveguide tuned 280-420 GHz

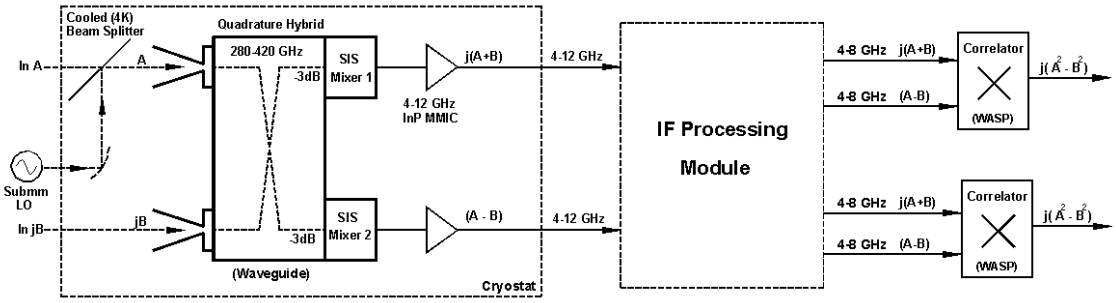

Figure 3. Block diagram a continuous comparison (correlation) receiver. Only one of the the polarizations is shown.

receiver. Further advantages result from the 8 GHz bandwidth, compared to the present 1 GHz. The 280-420 GHz band is chosen, not only because of the astronomical opportunities, but also because there is no shortage of local oscillator power to pump eight junctions (each SIS device has two tunnel junctions), waveguide techniques work well here, atmospheric and optical loss is relatively low, telescope efficiency is high (74%), and it is judged most likely to provide search opportunities for redshifted CII lines (z=3.7 - 5.8).

It should be noted that yet more sensitivity, with a single dish system, may be obtained for point source detection, by (in addition to the above) also separating the sidebands. To achieve all this, 8 mixers and either 4 or 8 wideband backends, depending on the technique used, shall be required. Since there is good atmospheric transparency over much of the 280-420 GHz frequency band at the CSO, dual polarization and instantaneous on-off DSB detection is probably the better choice. In this case, 2 rather than 4 wideband backends may be used. Moreover, it has been shown (Lamb *et al.*[11]) that the actual advantage gained by separating the sidebands very quickly diminishes in any real (lossy), non-zero temperature system.

For these reasons, the decision has been made to use only four mixers and two wideband spectrometers, configured in a correlating mode. Correlation is very important for rejecting gain variation, which is the primary problem facing wideband detection with SIS receivers. The gain in sensitivity is $\sqrt{2}$ for both polarizations, at least $\sqrt{2}$ for both on and off detection (depending on how much this suppresses gain variation effects). Given an optical depth (τ_{atm}) of 0.1 at 345 GHz, a 74% main beam efficiency of the telescope, a DSB receiver noise temperature of 50K, and 100 MHz of spectral resolution, we estimate an RMS noise level of the order of 85 μK in 8 hours of integration time. This assumes that the noise integrates down perfectly with root time, which is definitely not the case for the existing receivers.[37]

$T_{sys}(SSB)$ for a single pixel can be estimated as:

$$T_{sys}(SSB) = 2 * \frac{(T_{rec}(DSB) + T_{atm} * (1 - e^{-A\tau_{atm}}) + T_{spill})}{\eta_{mb} * \eta_{spill} * e^{-A*\tau_{atm}}}. \quad (21)$$

Where η_{mb} represents the main beam efficiency (0.74), η_{spill}=0.95, T_{spill}=14 K, and A the airmass. Since

$$T_{atm} \approx 0.95 * T_{amb}, \quad (22)$$

and T_{amb} is typically 270K, we find from the radiometer equation,[12] that the rms noise of the correlation receiver equals $\approx$ 85 μK in 8 hours of integration time,

$$\sigma = \frac{T_{sys}(SSB)}{\sqrt{(n * B * \tau_{int})}}. \quad (23)$$

Here n=4, and is the expected improvement of the dual polarization correlation receiver over a single pixel receiver.

4. NEEDED TECHNOLOGY

Significant progress on the upgrade of the correlation receiver and sidecab instrumentation hardware and software has been made. To achieve the required sensitivity and bandwidth, many of the new components had to be developed "in house". A noted exception is the University of Chalmers InP based 2-3K cryogenic low noise amplifier.[15,16] In the next section, we briefly describe each of the following components:

- Tunerless Full-Height Waveguide Mixers with Large Fractional RF-Bandwidth,
- Quadrature Waveguide Coupler with Large Fractional RF-Bandwidth,
- Combined 4-8 GHz IF Matching Network, DC-Break, Bias Tee, and EMI Filter and Power Combiner,
- 4-8 GHz Low Noise Cryogenic Amplifier,
- 4-8 GHz IF Gain Modules,
- Allan Variance Study of SIS Receiver Instability,
- Comprehensive Computer Control of the Bias Electronics,
- New set of SIS Junctions.

4.1. Tunerless Full-Height Waveguide Mixers with Large Fractional RF-Bandwidth

Many waveguide probe transitions have been proposed over the years, most of which have RF bandwidths of less than 35%. To lower the input impedance, the majority of these designs require significant reductions in waveguide height. Unfortunately, reducing the height makes the machining of submillimeter and terahertz components difficult. It also increases RF loss, as the effects of poor surface quality are enhanced by the increased current density in the walls of the waveguide. Because nearly all mixer designs have some kind of integrated thin-film tuning structure, there is a need for an efficient waveguide to thin-film microstrip transition that covers at least one full waveguide band, and is also easily extendible to THz frequencies.

To date, the majority of SIS and HEB waveguide mixers have employed planar probes that extend all the way across the waveguide.[18,20] An important reason for the popularity of this kind of design is the convenience with which the active device can be biased and the IF signal extracted. Unfortunately, this kind of "double-sided" (balanced) probe exhibits a rather poor RF bandwidth ($\leq 15\%$), when constructed in full-height waveguide. When the height of the waveguide is reduced by 50%, the probe's fractional bandwidth improves dramatically to a maximum of about 33%.[19] These results can be understood in that the popular double-sided probe is essentially a planar variation of the well known Eisenhart and Khan waveguide probe.[20] Borrowing from Withington's assessment,[21] the real part of the probe's input impedance is influenced in a complex way by the parallel sum of individual non-propagating modal impedances, and as such, is frequency dependent. By reducing

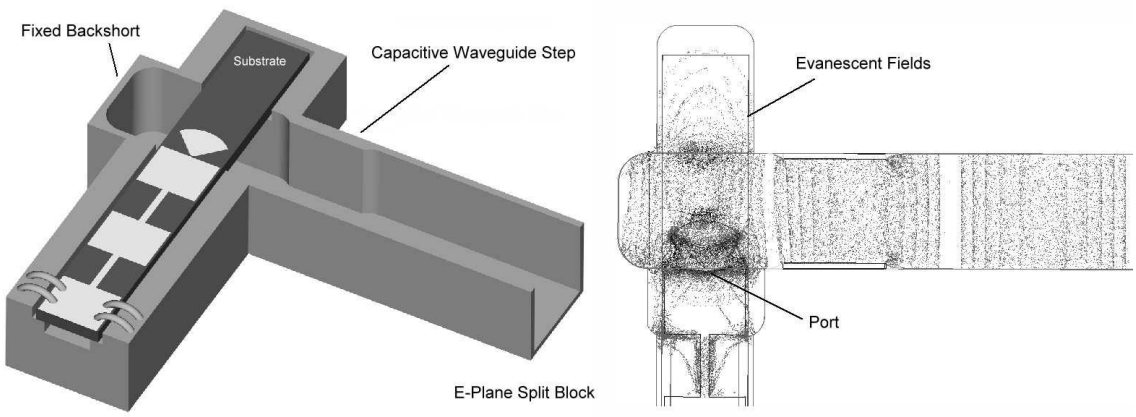

Figure 4. a) Inclusion of a capacitive tuning step in front of the radial probe. Though the physical size of the waveguide constriction is small ($\approx 15\%$), the reduction of the probe's input return loss and increase in bandwidth are dramatic. b) Electric field distribution in the waveguide and surrounding substrate material.

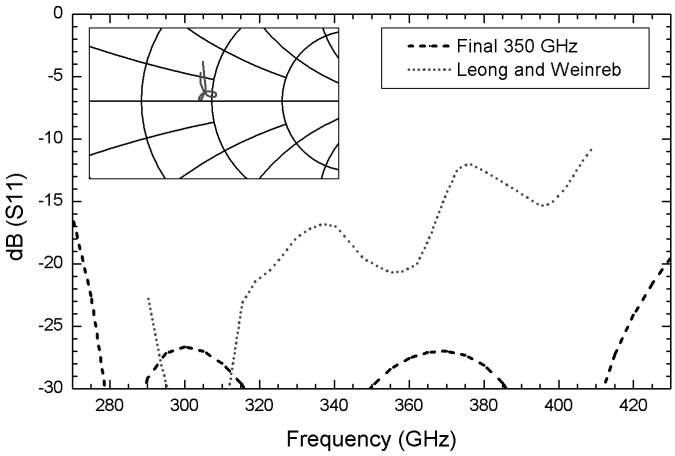

Figure 5. The predicted input return loss of a fixed tuned full-height SIS mixer block. Also shown is the predicted performance from a rectangular probe as reported by Leong and Weinreb *et al.* [17]. The fractional bandwidth of the 350 GHz full height waveguide radial probe is $\approx 45\%$. Refer to Table 2 and the text for details.

the height of the waveguide, the effects of the non-propagating modes can be reduced, which has been done very successfully, for example, by Tong and Blundell *et al.*.[19]

An alternative approach, is to use an asymmetric probe that does not extend all the way across the waveguide. For this kind of probe, referred to from now on as a "one-sided" probe, the modal impedances add in series. The real part of the input impedance is due to only the single propagating mode, and is relatively frequency independent.[21] These probes are typically implemented in full-height waveguide, which minimizes conduction loss and reduces the complexity of fabrication. Although a rectangular version of the "one-sided" probe has been used quite extensively by microwave engineers[22,23] and was introduced to the submillimeter community by Kerr *et al.*[24] in 1990, it is fundamentally different from the proposed radial-shaped probe. The radial probe described here represents an attempt to extend the use of radial modes (known to give superior broad band performance in thin-film microstrip radial tuning stubs, as compared to rectangular stubs) to the microstrip to waveguide coupling problem. From a practical point of view, the radial probe can be quite naturally made to feed a thin-film microstrip or cpw line that has a small line width and thin insulator. In the case of a rectangular probe, there would be a large geometrical discontinuity. Experimentally, we have found radial probes, implemented in the described thin-film configuration, give vastly superior performance over the more traditional approach. In 1999, Withington *et al.*[25] presented an extensive theoretical analysis of a "one-sided" rectangular probe in full-height waveguide.[23,24] We have followed this line of thought and implemented the mixers chips with the "fullheight" waveguide radial probe configuration.

If very broad band operation is required, a dramatic improvement in the probe's performance can be achieved by adding a simple capacitive waveguide tuning step, just in front of the probe. The added capacitive element collapses the characteristic probe impedance locus into a tiny "star", as shown in Fig. 5. Fig. 4 shows a diagram of a probe with the waveguide capacitive tuning step added. Typically, a 15% reduction in waveguide height is adequate to tune out most of the probe's residual impedance variation. The length of the step is of the order of the height dimension of the waveguide. Because some of the reactance in the probe is tuned out by the step, the distance between the substrate and backshort must be increased slightly: ($\Delta \approx 0.03$-$0.04\%\ \lambda_g$). This increase in distance represents an added advantage to using a waveguide step, as it eases machining tolerances. Chamfered corners in the waveguide have no effect on the overall performance of the probe, as long as the position of the backshort is compensated for accordingly. Finally; the capacitive waveguide step does not affect the impedance locus of the probe.

4.2. Quadrature Waveguide Coupler with Large Fractional RF-Bandwidth

As discussed, for the balanced and correlation receivers to work, either a 180° or 90° phase shift is needed between the input ports. Due to ease of fabrication we decided to use a 90° branch line waveguide coupler. The design is based on a narrower bandwidth split block version, developed for the ALMA project by Claude and Cunningham *et al.*[29].[30] Design and optimization of the wideband quadrature hybrid coupler were carried out in HFSS.[31] From 280-420 GHz, the coupled power imbalance is 0 ± 0.75 dB, while the predicted phase imbalance is less than $90 \pm 2°$. Design parameters are compiled in Table 3, and the predicted performance is shown in Fig. 7.

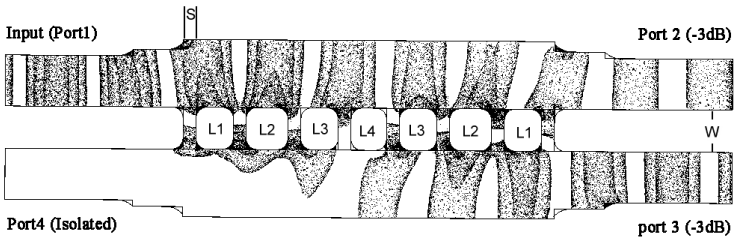

Figure 6. Electric field distribution in the quadrature waveguide coupler. The phase difference between port 2 and 3 is 90 ± 1.5 °.

Table 1. Hybrid Coupler Parameters used in Fig. 7

a-dim (μm)	**b-dim** (μm)	**S** (μm)	**L1** (μm)	**L2** (μm)	**L3** (μm)	**L4** (μm)	**W** (μm)
680	270	74	205	231	205	191	201

S denotes the branch line width, L the length between the branch lines, and W the separation between the two waveguides.

In order to achieve the required bandwidth, phase, and coupling it was necessary to maximize the number of branch lines (n). It was observed that:

$$n * S = \frac{\lambda_g}{2}. \tag{24}$$

Where n denotes the number of coupling sections.

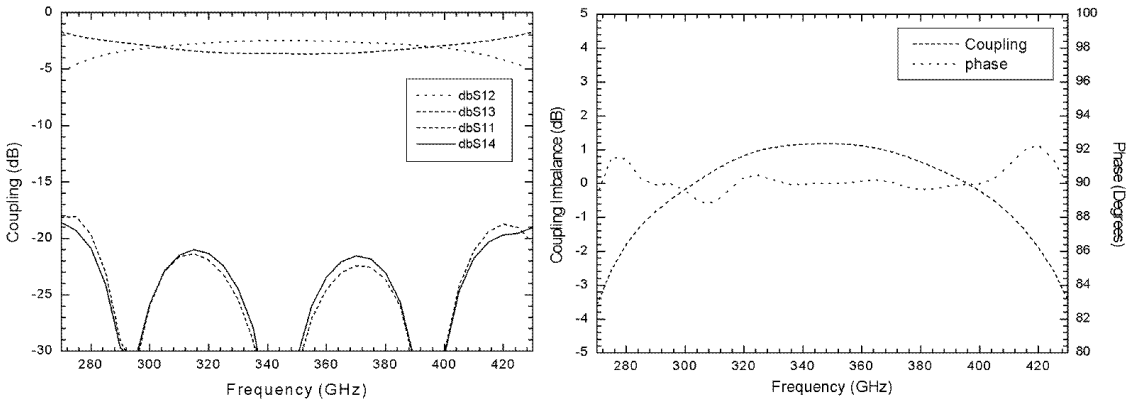

Figure 7. a) Predicted coupling performance. b) Delta phase and power imbalance of the quadrature hybrid coupler.

In order to achieve a practical mechanical design we decided, after consultation with Custom Microwave Inc.[33] to fix the width of the branch (air) lines to $\approx 74\mu$m. This then determined the number of coupler branches for each frequency band. To maximize the width of the branch lines, the waveguide width (b-dimension) of the coupler has been increased by a 32.5%. Increasing the waveguide width beyond this excites the next higher mode, thereby degrading the high frequency performance of the coupler. The separation of the two waveguides is $\approx\lambda_o/4$, as measured at the center of the band.

4.3. Combined 4-8 GHz IF Matching Network, DC-Break, Bias Tee, EMI Filter, and Wilkinson in Phase Power Combiner

In a practical mixer configuration, the device is terminated into a desired IF load impedance, the bias lines EMI filtered and injected via a bias Tee, and the IF output DC-blocked. DC blocking is usually accomplished with a small capacitor, by means of either a soldered contact or with wire bonds. Unfortunately, series resonance of physical capacitors are, by design, often located very near the edge of the IF band. Moreover, since the DC-blocking capacitor passes the mixer IF output, failure will be catastrophic. Indeed, component failure can occur in may ways. The most obvious case is perhaps stress due to repeated thermal cycling. As a viable alternative, we investigated the use of parallel coupled suspended microstrip lines.[34–36] As shown in Fig. 8, the suspended coupled microstrip lines act as a compact bandpass filter. For this filter to work, the ground plane directly

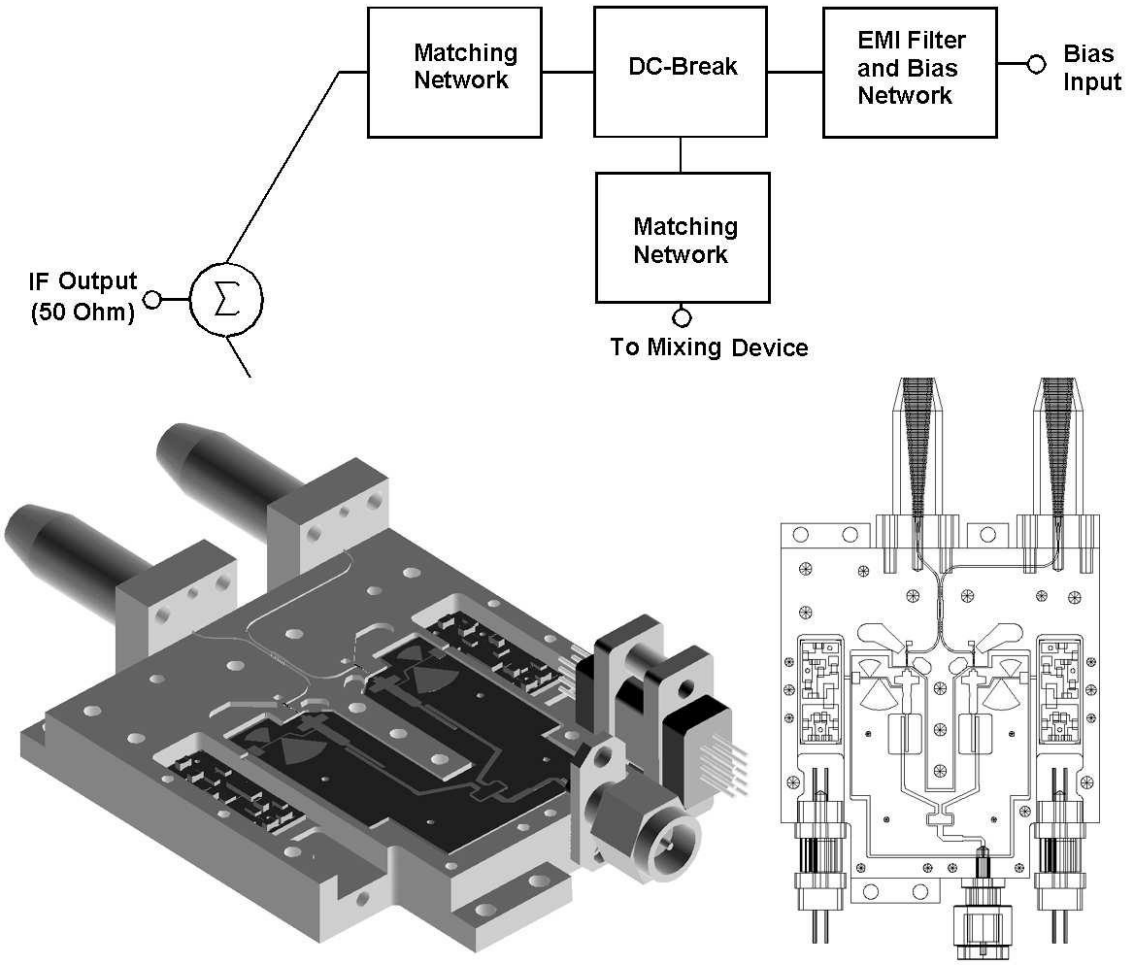

Figure 8. Balanced mixer block layout. The combined combined IF match, DC-break, Bias tee, EMI filter, and Wilkinson power combiner are planar by design. The E-field component of the incoming signal is horizontally polarized. Josephson noise suppression in the SIS tunnel junctions is accomplished by independent (not shown) controllable magnetic fields.

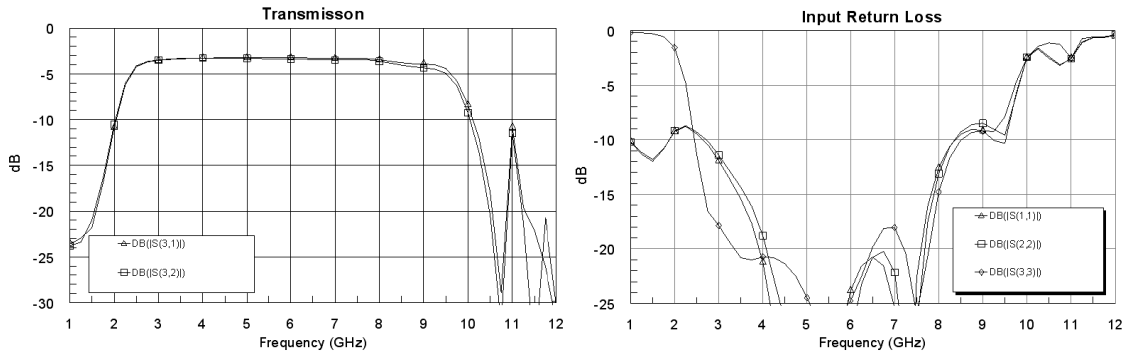

Figure 9. a) Coupled Power from the IF to the 20 Ω SIS junction port(s). Available bandwidth is 3-9 GHz, which is well in excess of the planned 4-8 GHz IF. Phase response (not shown) is within 0 ±1.5 degrees. b) Input return loss of the SIS and IF ports. The IF impedance at the SIS ports are kept low(20 Ω) in order to minimize noise saturation problems in the actual SIS tunnel junctions.

underneath the filter has been removed, and the IF board positioned on top of a machined cutout (resonant cavity). There are several discontinuities in this structure. When combined, they form the bandpass filter poles. The advantages are, simplicity of design (only one lithography step), and significantly improved reliability. The disadvantage, in some cases, may be its size, $\lambda_g/4$.

Details of the blocking filter are summarized in Table 2. The spacing S, and cavity depth HC set the coupling. Their tolerance values should be held to ± 5%. In the balanced mixer design presented in this paper, the SIS junctions are biased in opposite polarity (Fig. 1). This has the advantage that the IF currents may be summed in phase, which is readily achieved with an in phase Wilkinson power combiner.[4] The design presented here is entirely planar, the only component being a 100 Ohm thinfilm balancing resistor. This is a 1% laser trimmed NiCr resistor, fabricated directly onto the alumina IF circuit board.[32] In the design, we have made extensive use of HFSS,[31] a 3-D electro-magnetic field circuit simulator. The most important performance curves are depicted in Fig. 9.

Table 2. Coupling Parameters of Fig. 8

Substrate	**Er**	**Hsub** (μm)	**W** (μm)	**L** (mm)	**S** (μm)	**Hcav** (μm)	**Hair** (mm)	**Lc x Wc** (mm)
Alumina	9.80	635	480	5.72	120	585	2.5	5.08 x 6.1

H_{sub} denotes the substrate height, W the width of the coupled lines, L their length, S the spacing, H_{cav} the cavity depth, H_{air} the air height above the subtrate, W_c the cavity width, and L_c the cavity length. Center frequency is 6 GHz

4.4. 4-8 GHz Low Noise Cryogenic Amplifier

In collaboration with Chalmers University in Sweden and NASA's Jet Propulsion laboratory, we have acquired extremely low noise (2-3K) 4-8 GHz Indium Phosphide (InP) cryogenic low noise HEMT amplifiers.[15,16] The DC power consumption and input return loss of these amplifiers are excellent, ≈ 10 mW and -18 dB respectively. This means that the amplifier can be mounted on the LHe stage, and that cryogenic isolators may not be needed (though they are available commercially from Pamtek[17]). The amplifier gain is ≈ 25 dB (2 stages), and we are considering the use of low input return loss MMIC's for some additional cryogenic amplification.

4.5. 4-8 GHz IF Gain Modules

Room temperature amplification is accomplished by means of custom designed, CTT Inc.[38] fabricated and tested, gain modules. The overall gain of these modules is variable up to 60 dB, the in band gain flatness ± 1.5 dB, the input return loss ≤ 15 dB, and the noise figure 2.8 dB.

4.6. Allan Variance Study of SIS Receiver Instability

To achieve the required 85 μK of noise (100 MHz resolution BW), it is absolutely essential to understand (and minimize) causes of receiver instability. In 2000 we undertook such a study,[37] and many of the findings have been incorporated in the designs presented here.

4.7. Comprehensive Computer Control of the Bias Electronics

Control of the new receivers will be much simpler than with the existing tuned waveguide receivers; nevertheless, there are a lot of parameters that will need to be set (or optimized). To automate these tasks, we are developing the hardware and software that will allow near total automation of the tuning process. An added advantage is that the instruments can then be accessed remotely, if problems were to arise.

The electronics consists of a set of mixed signal bias cards and a custom data collection and command card which communicates with the electronics chassis computer. Each mixed analog/digital bias card is responsible for a separate function of the receiver electronics. These functions include: Biasing the SIS junctions and low noise amplifiers, setting magnetic field to suppress Josephson oscillations in the junctions, controlling and monitoring warm IF gain modules,[38] and setting the bias of the local oscillators. Each bias card has an FPGA that accepts commands to set voltages and currents via digital potentiometers, and transmit data from ADCs that measure multiple bias points.

Fundamentally, each card's FPGA sends and receives data on a SPI bus. The SPI bus can be shutdown when no command or data transfer is requested. Therefore, no digital edges (noise) occur when the bias points are set. As a added plus, the computer control of the multi-function cards can be placed as far away as the SPI interface permits. These features allow for quiet operation of the mixed analog/digital signal function bias cards once the receiver(s) is tuned.

Data and commands to/from the bias cards are sent over multiple, daisy-chainable, SPI busses that connect to a custom designed digital card, which in turn physically connects to a PCI bus inside the chassis mounted electronics server computer. It is the custom designed digital card that collects the data and commands packages of data to be sent over the computer internal bus, where remote access of the data via ethernet is possible. The custom digital card also sends commands from the electronics computer to the appropriate multi-function bias cards, and henceforth control of all receiver bias functions is indirectly possible over ethernet. To control the hardware, software has been developed to transmit data and commands over the ethernet to facilitate remote control of the electronics. Part of the software package resides on the chassis mounted electronics computer, the other half being distributed to the remote control computer communicating with the receiver computer.

4.8. New set of SIS Junctions

Circuit designs of high current density niobium based SIS junctions (4 bands) were submitted to JPL in spring 2003 for fabrication. Since that time they been fabricated, lapped and diced. The new SIS tunnel junctions all share the same 50 μm thick Quartz wafer. The junction design employs twin SIS junctions with AlN barriers and a RnA product of 7.6 $\Omega \cdot \mu m^2$ (Jc=35 kA/cm^2 current density). Supermix,[7] a flexible software library for high-frequency superconducting circuit simulation has been used exclusively in the design process. The predicted balanced mixer results described in this section are derived from (harmonic balanced) superconducting SIS mixer simulations in combination with extensive 3D em-field (HFSS) analyses of the RF and IF mixer circuitry (Sections

Figure 10. 350 GHz Junction layout. The radial probe antenna is visible on the left side. The IF is taken out via a microstrip RF choke (on 300 nm SiO, ϵ_r=5.6) which connects to a high impedance CPW transmission line (inductive) and shunt capacitor. This LC mechanism provides a π tuning network with the combined capacitance of the Probe, twin junction RF tuning structure, and microstrip RF choke. The IF passband of mixers under discussion has been optimized to cover 1-13 GHz.

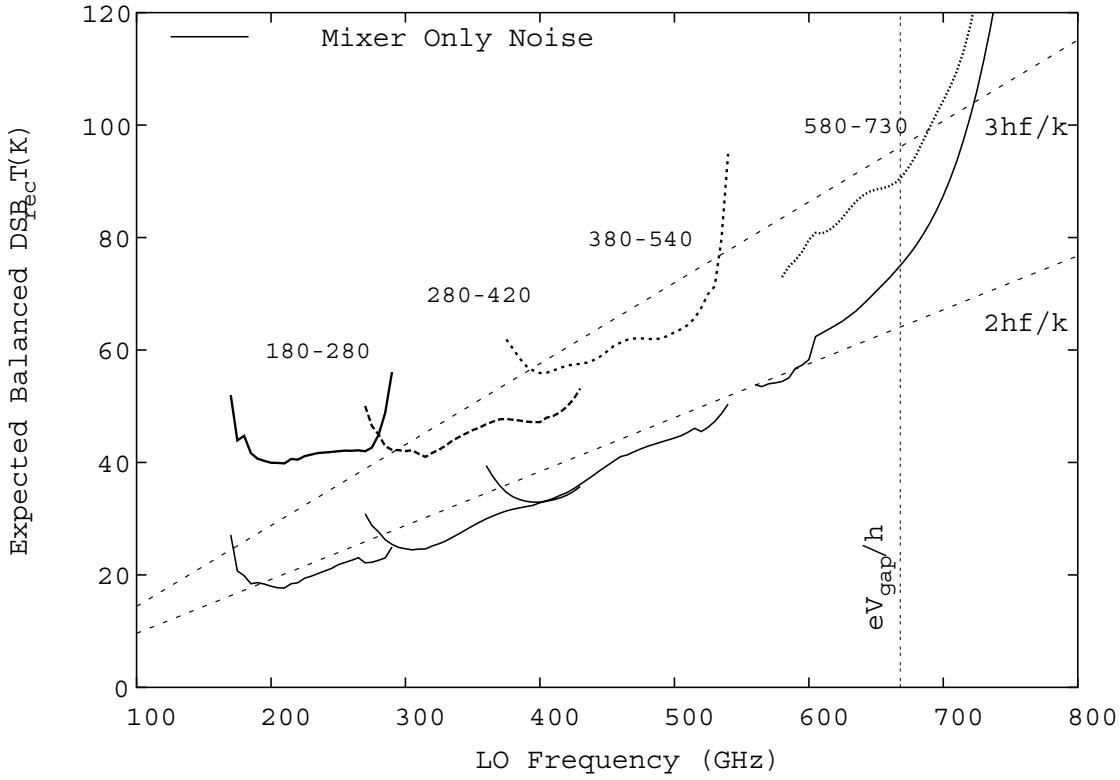

Figure 11. Estimated double side-band receiver noise temperatures for the balanced mixers constructed of junctions 'A' and 'B' (see I-V and gain characteristics in Fig. 12). The noise estimate was calculated by supermix[7], and uses detailed 3D em-field analyses of the RF hybrid, IF-match and summing node, and includes 5K IF noise accounting for LNA and isolator, and a realistic optics model for dual band receivers. The LO noise contribution is minimal thanks to the noise rejection properties of the balanced mixers (calculated to be $\approx$ 11 dB), and the fact that the LO is injected via a cooled ($\approx$ 10 dB) attenuator. Beneath is plotted the mixer only noise temperatures that may be used to estimate receiver temperatures for different IF and optics configurations.

4.1-4.4). This may well be the first time that a superconducting mixer of this complexity has been simulated in it's entirety.

Both RF and IF matching is realized on chip, yielding a flat IF response out to high (> 13 GHz) IF frequencies. All designs have been optimized for maximal conversion gain and minimal noise temperatures across the entire operational band. In Fig. 11, we show the (calculated) balance receiver and mixer noise temperature from 180-720 GHz in 4 waveguide bands. To obtain a realistic estimate of the receiver noise, we used the measured optics losses of the present receivers minus the LO noise. The LO noise contribution may be neglected due to the noise rejection properties of the balanced mixer (calculated to be $\approx$ 11 dB), and the fact that the LO is injected via a cooled 10 dB attenuator. From Fig. 12 it is evident that the mixer gain, even under $\pm$ 1 dB LO pump power mismatch is tolerable. This is important since it means that the individual SIS junctions may be biased at the same voltage setting. The designs have also been checked for IF saturation. Supermix has furthermore been used to determine optimal bias and pumping conditions, while at the same time avoiding instability in the SIS mixer. Instability can result in increased RF and IF reflection, which in turn is likely to cause poor baseline subtraction (data). These optimal values can be set by the computer controlled bias electronics as discussed in Section 4.7.

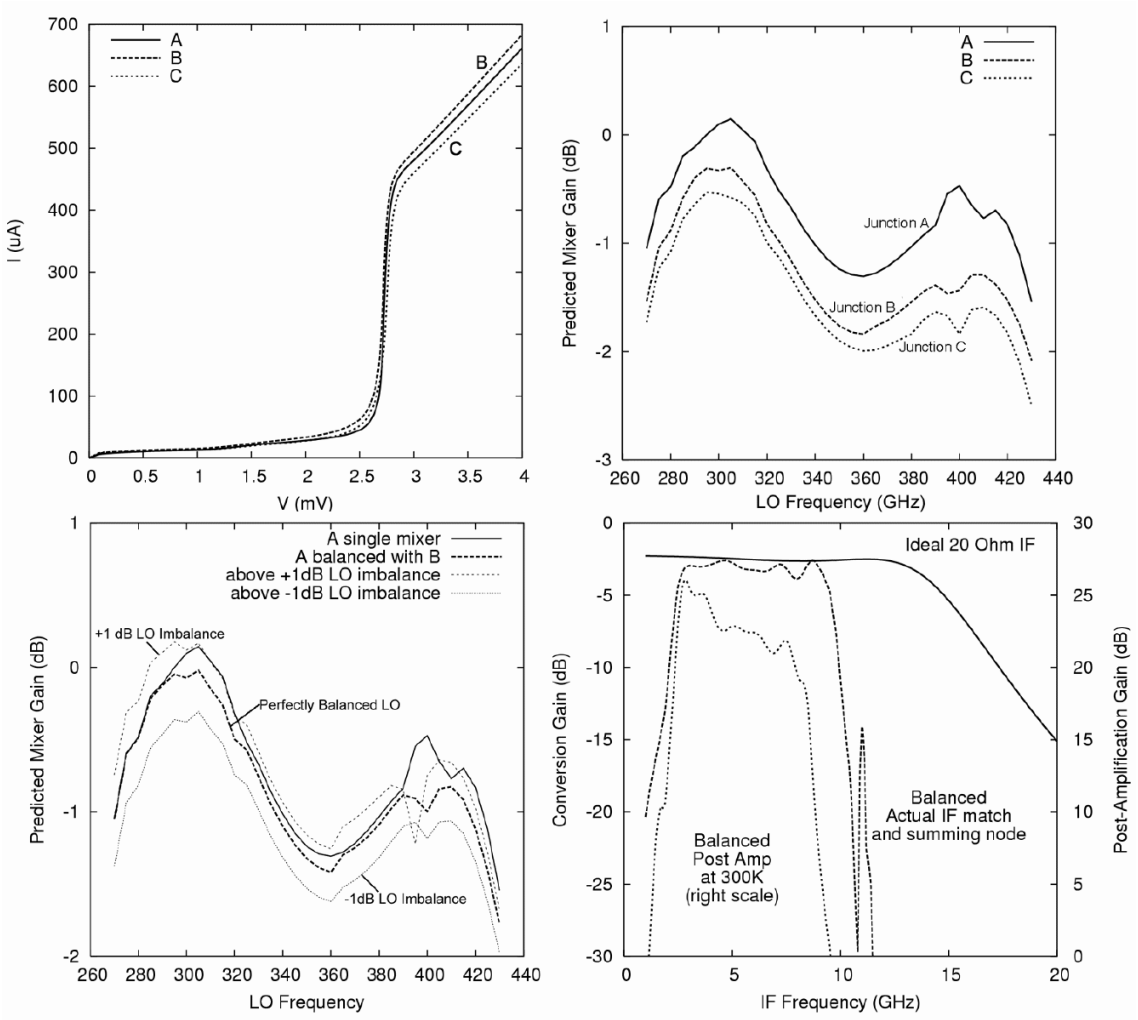

Figure 12. a) Three typical measured I-V curves from wafer B030926. The junction characteristics are reasonably well matched, with slight variations in the definition of the gap area, affecting the mixer gain performance (Fig. 12b, c). In case of the 600-720 GHz receiver, the gap voltage though being a bit low does not appear to significantly impact the mixer noise performance. b) Estimated conversion gain with the mixer tuned for optimal noise performance. As expected, junction 'A' with the sharperst gap provides the best conversion gain, and hence the lowest noise temperature. Note that the variation among the three junctions is reasonably small (less than 1 dB). c) Mixer gain for a balanced configuration. Since a balanced set-up involves using two non-identical mixers, the questions is how much degradation of the mixer gain performance may be expected vs. a single mixer. For reference, the conversion gain of a single mixer is plotted for junction 'A'. Compare this result with the conversion gain of balanced mixer that uses both junctions 'A' and 'B'. A further limitation of the balanced design (Fig. 7) is that the LO power as a function of frequency is not equally split between the two junctions. This arrangement under a typical $\pm$ 1 dB LO pumping imbalance is also shown here. From Fig's 12a-c, we may conclude that gain imbalanced due to 1) device characteristics, and 2) LO power imbalance is not expected to significantly effect the overall balanced mixer performance (Fig. 11). d) Expected IF throughput at a LO frequency of 350 GHz. It is apparent that the SIS junctions (Fig. 10) produce a flat gain from 0-13 GHz, assuming an ideal 20 Ohm termination. In case of the CSO balanced mixers, the specified mixer IF passband is 4-8 GHz. Based on extensive HFSS simulations, the IF match (Section 4.3) provides a good match into 50 Ω from 2.5-9.5 GHz. The actual receiver bandwidth is limited however to 4-8 GHz by the cooled Isolator[17] and low noise (2K) Chalmers University amplifier[15]. In case of the correlation (Galaxy) receiver, the IF passband will be 4-12 GHz.

5. CONCLUSION

Upgrade plans to the Caltech Submillimeter Observatory (CSO) have been presented. In the near future, the existing DSB waveguide receivers will be upgraded with tunerless very large RF bandwidth balanced SIS mixers.

These receivers may be configured in a dual (2-color) observation mode, which will greatly improve science throughput and facilitate pointing for the high frequency receivers in mediocre weather. The IF for the new system is 4-8 GHz.

Balanced mixers have the distinct advantage that all the available LO power is utilized, which significantly reduces LO power requirements. In turn, this facilitates the use of very wide RF bandwidth tunerless LO's. An added benefit of this scheme is that LO noise is greatly reduced (estimated to be $\approx$ 11 dB in a practical submillimeter receiver). The issue of noise rejection is particularly relevant with the advent of synthesizer driven LO sources.

Finally, good progress has been made on the development of a 280-420 GHz continuous comparison receiver, for the detection of very faint (high-z) extragalactic sources. Much of the required hardware, needed for the new instrumentation has been developed at Caltech, and is either complete or has been submitted for fabrication. Installation of the new receivers is expected to commence in the winter of 2004. The actual upgrade may take several years, as all IF hardware at the telescope will need to be replaced, cryostats upgraded, and new interfacing software written.

6. ACKNOWLEDGEMENTS

We wish to thank Niklas Wadefalk for his help with the IF components, Martin Houde for his input on (thermally) stabilized IF amplification, and Richard Chamberlin for useful insights in the multitude of system related issues. This work was supported in part by NSF Grant# AST-0229008.

REFERENCES

1. R.Schieder, O.Siebertz, F.Schloeder, C.Gal, J.Stutzki, P.Hartogh, V.Natale, "Wide-Band Spectrometer for HIFI-FIRST", *Proc. of "UV, Optical,* and IR Space Telescopes and Instruments", J.B. Breckinridge, P.Jakobsen Eds., SPIE 4013, 313-324, 2000.
2. R.Schieder, J.Horn, O.Siebertz, M.Klumb, J.Frerick, V.Tolls "Acousto-Optical Spectrometers in Space", *The 30th ESLAB Symposium on Submillimetre and Far-Infrared Space Instrumentation,* ESTEC, Noordwijk, The Netherlands, Sept. 24-26, 1996, ESA SP-388, 187.
3. J.Horn, O.Siebertz, F.Schmilling, C.Kunz, R.Schieder, G.Winnewisser; "A 4X1 GHz Array Acousto-Optical Spectrometer", *Experimental Astronomy* Vol. 9, 17-38, 1999)
4. E.J. Wilkinson, "An N-way Hybrid Power Divider", *IRE, Microwave Theory and Techniques,* Vol MTT-13, January 1960, pp. 116-118.
5. A. I. Harris, and J. Zmuidzinas, "A Wideband Lag Correlator for Heterodyne Spectroscopy of Broad Astronomical and Atmospheric Spectral Lines" "*Rev. Sci. Instrumentation,* Vol 72, No. 2, pp. 1531-1538, 2001
6. A. I. Harris, *Proceedings of SPIE, Millimeter and Submillimeter Detectors,*Kona, HI. 2002.
7. J. Ward, F. Rice and J. Zmuidzinas, "Supermix: a flexible software library for high-frequency circuit simulation, including SIS mixers and superconducting components", *Tenth International Symposium on Space Terahertz Technology,* University of Virginia, Charlottesville, VA, March 1999.
8. S.A. Maas, Microwave Mixers, 2^{nd} Edition.
9. Virginia Diodes Inc. 321 West Main Street, Charlottesville, VA22903, USA.
10. C.R. Predmore, N. R. Erickson, G.R. Huguenin, and P. Goldsmith, "A Continuous Comparison Radiometer at 97 GHz" *IEEE, Microwave Theory and Techniques,* Vol MTT-33, No. 1, January 1985.
11. J.Lamb "SSB vs. DSB for Submillimeter Receivers", *Alma Memo 301.*
12. J.D. Kraus, "Radio Astronomy", *2nd Edition, pp7-8*
13. J.W. Kooi, G. Chattopadhyay, S. Withington, F. Rice, J. Zmuidzinas, C.K. Walker, and G. Yassin, "A Full-Height Waveguide to Thin-Film Microstrip Transition with Exceptional RF Bandwidth and Coupling Efficiency" *Int J. IR and MM Waves,* Vol. 24, No. 3, Sept, 2003.
14. M. L. Edgar and J. Zmuidzinas, "CASIMIR, a Submillimeter Heterodyne Spectrometer for SOFIA" *Proceedings of SPIE, Airborne Telescope Systems,* Vol. 4014, pp. 31-42, Munich, Germany 2000

15. N. Wadefalk, A. Mellberg, I. Angelov, M. Barsky, S. Bui, E. Choumas, R. Grundbacher, E. Kollberg, R. Lai, N. Rorsman, P. Starski, J. Stenarson, D. Streit, and H. Zirath, "Cryogenic, Wide-band, Ultra-low-noise IF Amplifiers operating at Ultra-Low DC-Power," *IEEE, Trans. Microwave Theory and Techniques,* Vol. 51, No. 6, pp. 1705-1711, June 2003.
16. Private Communication.
17. Pamtek 4053 CalleTesoro, Camarillo, Ca 93012, USA.
18. J. W. Kooi , M. Chan, B. Bumble, and T. G. Phillips, "A low noise 345 GHz waveguide receiver employing a tuned 0.50 μm^2 Nb/AlO_x/Nb tunnel junction," *Int. J. IR and MM Waves,* Vol. 15, No. 5, May 1994.
19. Tong C-Y. E., Blundell R, Paine S, "Design and characterization of a 250-350-GHz fixed-tuned superconductor-insulator-superconductor receiver", *IEEE, Microwave Theory and Techniques,* Vol MTT-44, pp. 1548-1556, Sept. 1996.
20. R. L. Eisenhart and P. J. Khan, "Theoretical and experimental analyses of a waveguide mounting structure", *IEEE, Microwave Theory and Techniques,* Vol MTT-19, pp. 706-717 (1971).
21. S. Withington, and G. Yassin, "Analytical expression for the input impedance of a microstrip probe in waveguide," newblock*Int. J. IR and MM Waves,* Vol. 17, pp. 1685-1705, Nov. 1996.
22. Y-C Leong, and S. Weinreb "Full-band Waveguide-to-microstrip probe transitions" *IEEE, Microwave Theory and Techniques,* Digest of Papers, Anaheim, CA, June 13-19, 1999.
23. J.H.C. van Heuven "A new integrated waveguide-microstrip transition", *IEEE, Microwave Theory and Techniques,* Vol MTT-24, pp. 144-147, March 1976.
24. A. R. Kerr and S. K Pan, "Some recent developments in the design of SIS mixers,", *Int. J. IR and MM Waves,* Vol. 11, No. 10, pp. 1169-1187, Nov. 1990.
25. S. Withington, G. Yassin, J. Leech, and K. G. Isaak, "An accurate expression for the input impedance of one-sided microstrip probes in waveguide", *Tenth International Symposium on Space Terahertz Technology,* Charlottesville, March 1999.
26. E. Schelecht, G. Chattopadhyay, A. Maestrini, A. Fung, S. Martin, D. Pukala, J. Bruston, and I. Mehdi, "200, 400, and 800 GHz Schottky diode substrateless multipliers: Design and Results" *2001 IEEE, MTT-S International Microwave Symp. Digest,* Phoenix, Az, pp1649-1652, May 2001.
27. J.W. Kooi, J. Pety, B. Bumble, C.K. Walker, H.G. LeDuc, P.L. Schaffer, and T.G. Phillips, "A 850 GHz Waveguide Receiver employing a Niobium SIS Junction Fabricated on a 1μm Si_3N_4 Membrane," *IEEE Transactions on Microwave Theory and Techniques,* Vol. 46, No. 2, pp151-161, February 1998.
28. J. W. Kooi, C.K. Walker, J. Hesler, "A broad band suspended membrane waveguide to microstrip transition for THz Applications," *9th International Conference on Therahertz Electronics,* University of Virginia, Oct. 15-16, 2001.
29. S.M.X Claude and C.T. Cunningham, "Design of a Sideband-Seperating Balanced SIS Mixer Based on Waveguide Hybrids," *Alma Memo 316,* September 2000
30. C.C. Chin, D. Derdall, J. Sebesta, F. Jiang, P. Dindo, G. Rodrigues, and D. Bond, "A Low Noise 100 GHz Sideband-Separating Receiver," *Int J. IR and MM Waves,* Vol. 25, No. 4, May, 2004
31. Ansoft Corporation Four Station Square, Suite 200, Pittsburgh, PA 15219-1119, USA
32. American Technical Ceramics One Norden Lane, Huntington Station, NY 11746, USA
33. Custom Microwave Incorporated Custom Microwave, Inc., 940 Boston Avenue Longmont, CO 80501, USA.
34. W. Menzel, L. Zhu, K. Wu, F. Bögelsack Compact Broadband Planar Couplers, *31st European Microwave Conference,* London, UK, Sept. 25-27, 2002.
35. G. de Lange, SRON, NL, Private Communication
36. H. Golstein, SRON, NL, Private Communication
37. J.W. Kooi, G. Chattopadhyay, M. Thielman, T.G. Phillips, and R. Schieder, "Noise Stability of SIS Receivers," *Int J. IR and MM Waves,* Vol. 21, No. 5, May, 2000
38. CTT Incorporated 3005 Democracy Way, Santa Clara, CA 95054, USA